

# Analysis and Modeling Method of Mechanical Behavior Based on Trampoline Movement

Junzhe Tang<sup>1\*</sup>, Yumeng Li<sup>1</sup>, Chuhan Wang<sup>1</sup>, Yongfang Shi<sup>1</sup>, Kewei Huang<sup>1</sup>

<sup>1</sup>Xianda College of Economics and Humanities, Shanghai International Studies University, Shanghai, 200080, China

\*Corresponding Author

## Abstract

Trampoline gymnastics is a high-difficulty sport integrating explosive power, coordination, and precise control. To scientifically guide training protocols and extend equipment service life, this study establishes a multi-phase mathematical model covering the entire trampoline motion process, sequentially addressing athlete takeoff posture optimization, landing impact buffering control, and multi-athlete collaborative jump fatigue analysis.

This study establishes a biomechanical model to analyze the direction, magnitude, and relationship between force application and body posture of a 1.75-meter-tall athlete performing a standardized forward somersault during the takeoff instant. Numerical simulation is employed to validate the model's rationality. A force exertion posture analysis model based on rigid body dynamics and angular momentum conservation was developed to resolve "how to achieve front flips by adjusting takeoff direction and body posture." By constructing a nonlinear mapping model linking exertion angle, angular velocity, and maneuver completion, the minimum required take off angle ( $17^{\circ}$ – $20^{\circ}$ ) for standard flips was identified. Analysis of posture control strategies for athletes of different body types revealed that medium angles ( $17^{\circ}$ – $20^{\circ}$ ) represent an ideal range balancing maneuver completion and force efficiency.

Dynamic equations are formulated to characterize the forces acting on the athlete from takeoff to landing, determining the landing velocity and impact forces. Without considering the athlete's center of gravity, strategies for minimizing impact forces through adjustments in takeoff height and landing posture are investigated. A landing impact dynamics model centered on a mass-spring-damper system was constructed to address "how to mitigate landing impacts and enhance safety." By solving nonlinear ODE systems simulating the complete takeoff-flight-landing process, nine landing strategies were evaluated via numerical simulations. The optimal buffering strategy reduced peak impact forces from 4,018 N to 2,847 N, achieving a 29.1% reduction and significantly improving safety performance.

A multi-athlete dynamic model incorporating variables such as body weight and takeoff timing is developed to analyze the stress distribution and fatigue damage of the trampoline under varying conditions. An optimization strategy minimizing fatigue damage is proposed based on weight distribution and synchronized takeoff sequences, with predictions of fatigue life improvement before and after implementation.

A trampoline impact-fatigue evolution coupling model under multi-athlete collaborative conditions was established by integrating fatigue accumulation theory and takeoff sequence optimization. Simulation results indicated that the original sequence achieves local optimization under current settings, but the model can be extended to intensive-use scenarios. Through dynamic scheduling of body weights and take off sequences to avoid force peak superposition, equipment fatigue is markedly delayed.

In summary, this study constructs a comprehensive mechanical analysis framework spanning individual force modeling, motion buffering control, and multi-athlete weight-sequence coordination. It proposes quantifiable, optimizable, and generalizable training strategies and structural lifespan management methods. The developed models exhibit strong universality and interpretability, applicable to competitive training, equipment design, and fatigue assessment scenarios.

Keywords

Trampoline Dynamic System Modeling, Rigid Body Rotational Dynamics , Ground Impact Attenuation Optimization, Structural Fatigue Life Prognostics, Time-Sensitive Control Policy Optimization

1. Introduction

During the competition, an athlete with a height of 1.75 m (other parameters see Appendix Table 1) completes a full "forward somersault" maneuver according to regulations. Analyze the direction and magnitude of the force exertion required by the athlete at the instant of take-off to execute this maneuver, and the relationship between this force exertion and the athlete's body posture. Establish a corresponding model and consider employing numerical simulation methods to validate the model's reasonableness.

Analyze the forces acting on the athlete during the airborne flight phase after take-off from the trampoline and during the landing process. Establish the kinetic equations governing the athlete's motion from take-off to landing, determining the athlete's velocity and force conditions at the moment of landing. Without considering the athlete's center of mass, further discuss how adjustments to take-off height and landing posture can reduce the impact force upon landing.

Assumption: The athlete begins descending upon reaching the peak of the trajectory. During descent, consider the following two factors:

- The effect of aerodynamic drag on the athlete.
- The elastic recovery characteristics of the trampoline at the instant of landing.

If multiple athletes perform trampoline movements simultaneously, establish kinetic equations incorporating variables such as individual body weights and take-off times. Analyze the force conditions on the trampoline and the degree of fatigue damage under different scenarios. Considering factors such as the weight distribution of multiple athletes (see Table 1) and the take-off timing sequence (all athletes must take off before any landing occurs), propose a strategy to minimize trampoline fatigue damage. Predict the enhancement effect on the trampoline's fatigue life before and after implementing the proposed strategy.

Table 1: Basic parameters and positions of athletes

Athlete ID	Gender	Height (m)	Lower Limb Length (m)	Body Mass (kg)	Standing Position Coordinates (x, y)	Center of Mass Height Above Ground (m)	Local Trampoline Vertical Stiffness Coefficient (N/m)
1	Male	1.75	(2.0, 1.0)	0.88	68	about 0.93m	4951.05
2	Female	1.63	(3.8, 0.5)	0.81	55	about 0.84m	4932.36
3	Male	1.80	(1.2, 1.5)	0.90	72	about 0.95m	4970.56
4	Female	1.68	(0.8, 1.8)	0.84	60	about 0.86m	4973.62
5	Male	1.70	(3.0, 1.2)	0.85	65	about 0.88m	4935.29

## 2. Problem Restatement

Problem 1: This study establishes a biomechanical model to analyze the direction, magnitude, and relationship between force application and body posture of a 1.75-meter-tall athlete performing a standardized forward somersault during the takeoff instant. Numerical simulation is employed to validate the model's rationality.

Problem 2: Dynamic equations are formulated to characterize the forces acting on the athlete from takeoff to landing, determining the landing velocity and impact forces. Without considering the athlete's center of gravity, strategies for minimizing impact forces through adjustments in takeoff height and landing posture are investigated.

Problem 3: A multi-athlete dynamic model incorporating variables such as body weight and takeoff timing is developed to analyze the stress distribution and fatigue damage of the trampoline under varying conditions. An optimization strategy minimizing fatigue damage is proposed based on weight distribution and synchronized takeoff sequences, with predictions of fatigue life improvement before and after implementation.

### 2.1. Restatement of Problem 1

When executing high-difficulty trampoline maneuvers (such as a forward somersault), the athlete must generate sufficient vertical velocity and angular velocity through an effective ground push-off during the take-off phase to achieve both aerial elevation and body rotation. Problem 1 aims to investigate the direction and magnitude of the force applied by the athlete at the instant of take-off, and its relationship with body posture parameters (e.g., tilt angle). A dynamics model needs to be established to assess the kinematic feasibility of completing the maneuver under given conditions and to quantify the correlation between take-off posture and maneuver completion.

### 2.2. Restatement of Problem 2

When the athlete lands after completing the aerial maneuver, their body exerts a transient impact force on the trampoline bed. Problem 2 requires establishing a comprehensive dynamics model encompassing the entire sequence from take-off, through airborne flight, to the landing impact phase. This model will analyze the influence of different landing posture parameters (e.g., landing angle, knee flexion level) on the magnitude of the impact force and evaluate the impact mitigation performance of various landing strategies. The objective is to optimize landing parameters to minimize the peak impact force, thereby enhancing safety during training sessions.

### 2.3. Restatement of Problem 3

If multiple athletes perform trampoline exercises consecutively on the same apparatus, variations in movement rhythm and body mass can subject the structure to a sequence of high-intensity impacts within a short timeframe, leading to cumulative fatigue damage. Problem 3 requires establishing a multi-athlete coordinated jumping model. This model must incorporate individual take-off timing and spatial mass distribution to compute the trampoline's dynamic load variation and fatigue damage accumulation under different strategies. The objective is to minimize structural damage by optimizing the take-off sequence deployment and to predict the enhancement magnitude of fatigue life achievable under the optimized strategy.

## 3. Mechanical Analysis

### 3.1. Analysis of Problem 1

Problem 1 primarily focuses on the dynamic modeling of a single athlete during the take-off phase. The core variables include vertical velocity, angular velocity, force exertion direction, and

body posture. This problem constitutes a classic rigid body dynamics analysis task. By applying the principles of linear momentum conservation, angular momentum formulation, and torque calculation, a relationship can be established between the force application angle, the exerted force magnitude, and the resulting body rotation. The model must possess inverse modeling capability, meaning that for a given target maneuver (e.g., a single somersault), it should be able to derive the minimum required take-off angle and force exertion intensity necessary to successfully complete the maneuver.

### 3.2. Analysis of Problem 2

Problem 2 addresses the impact response within a nonlinear system, representing a quintessential modeling task for a spring-damper system. During landing, the athlete transfers their kinetic energy to the apparatus system. Consequently, the critical challenge lies in accurately simulating this transient impact process and controlling the energy dissipation rate through adjustments in landing parameters (e.g., knee flexion amplitude, body angle). The model should incorporate the solution of the governing dynamic equations and include parameter sensitivity analysis. It must output key performance indicators such as peak impact force magnitude and response duration to evaluate the effectiveness of different shock mitigation strategies.

### 3.3. Analysis of Problem 3

Problem 3 introduces elevated modeling complexity by extending the system from a single athlete to a multi-agent collaborative framework, integrating temporal sequence optimization and fatigue damage theory. The resultant forces on the system depend not only on individual actions but also on time-domain control parameters. The model must address nonlinear stress superposition, cumulative fatigue damage, and optimal scheduling strategies. The critical challenge lies in mapping the takeoff-landing events of multiple athletes into a temporal sequence of impulse loads and optimizing system response peaks (e.g., force maxima) and fatigue life metrics through strategy search algorithms (e.g., jump sequence optimization).

## 4. Model Assumptions

1. Rigid Body Assumption : In Problem 1, we model the athlete's body as a rigid body, neglecting internal biomechanical variations. During the take-off phase, changes in body posture depend solely on rigid-body rotation and center-of-mass displacement, without accounting for detailed muscle or joint kinematics.
2. Neglecting air resistance : Although aerodynamic drag affects the athlete's velocity during aerial phases in reality, this model assumes negligible influence of air resistance on motion dynamics for simplification.
3. Assumption of instantaneous take-off and landing impacts : In Problem 2, the model treats each athlete's landing impact as an impulsive force with infinitesimal duration, neglecting potential continuous force variations caused by finite contact time between the athlete and the surface.
4. Elastic and damping properties of the trampoline : In Problems 2 and 3, the elastic coefficient ( $k$ ) and damping coefficient ( $c$ ) of the trampoline are assumed to be constant and uniformly distributed. The trampoline surface is presumed to exhibit no nonlinear effects in its mechanical response, behaving strictly as a linear spring-damper system.
5. Non-conflicting multi-athlete take-off assumption : In Problem 3, all athletes are assumed to take off according to a predefined time sequence, with no overlapping jumps—each athlete must take off only after the preceding athlete has landed. This ensures that, at any given moment, only one athlete exerts force on the trampoline, preventing peak impact overlaps.

6. Fatigue damage assumption : In the fatigue damage modeling, the trampoline’s structural fatigue life is assumed to depend solely on the cumulative impact forces from landings, excluding other environmental factors (e.g., temperature variations, long-term material degradation).
7. Idealized jumping assumption : In Problem 1, the athlete’s take-off velocity and angular velocity are modeled under ideal conditions—free from technical errors or deviations in posture control.
8. Linear time-series model assumption : In Problem 3’s multi-athlete coordination analysis, each athlete’s take-off and landing behavior is treated as independent, unaffected by others. The model assumes a linear superposition of individual take-off times, body weights, and impact forces.

5. Nomenclature and Symbolic Definitions

Table 2: Different internship symbols and their corresponding definitions

Symbol	Definition
$m$	Athlete mass(kg)
$v_0$	Vertical velocity of the center of mass (CoM) at take offmass (CoM) at take off
$\omega_0$	Angular velocity about CoM at takeof
$F_t$	Magnitude of ground reaction thrust force
$\theta$	Thrust angle relative to vertical
$\alpha$	Angular acceleration
$F_d$	Aerodynamic drag force
$c$	Equivalent damping coefficient during landing
$F_r$	Landing rebound force
$m_i$	Mass of i-th athlete
$F_i(t)$	Force exerted by i-th athlete on trampoline
$N_f$	Theoretical fatigue life cycles (undamaged)

Continued Table 2: Different internship symbols and their corresponding definitions

Symbol	Definition
$\Delta\sigma$	Stress amplitude
$t_i^{jump}$	Takeoff time of i-th athlete
$t_i^{land}$	Landing time of i-th athlete
$\sigma(t)$	Instantaneous stress at a trampoline cross-section

## 6. Dynamical System Formulation and Numerical Implementation

### 6.1. Modeling and Solution for Problem 1

Trampolining, often termed "aerial ballet," critically depends on maximizing elastic energy conversion for effective flight height and mid-air control to execute complex maneuvers (e.g., somersaults). The take off phase is pivotal, requiring athletes to generate two essential quantities within 0.2–0.3 s:

1. Sufficient vertical velocity to propel the body into the air;
2. Appropriate angular velocity to achieve the required rotation angle (e.g., 360° corresponding to  $\pi$  radians).

This study focuses on modeling the force direction, magnitude, and their relationship with body posture during the take-off phase of a forward somersault performed by a 1.75 m tall, 68 kg male athlete. The objective is to mathematically characterize the biomechanical principles and motor control mechanisms underlying the take-off motion, providing a theoretical foundation for practical training and equipment optimization.

#### 6.1.1. Vertical Takeoff Dynamics

During the take-off phase, to propel the athlete's body upward, their center of mass must attain a certain initial vertical velocity ( $v_{z0}$ ). This vertical velocity is generated by the normal reaction force ( $F_n$ ) exerted by the feet against the trampoline bed, which can be analyzed using the impulse-momentum theorem:

$$F_y - mg = m \cdot \frac{v_0}{T} \Rightarrow F_y = mg + m \cdot \frac{v_0}{T} \quad (1)$$

In Equation (5-1),  $\frac{v_0}{T}$  represents the mean acceleration, and  $mg$  corresponds to the force required to counteract gravitational acceleration. This leads to the fundamental relationship: the greater desired jump height, the necessitates a larger vertical take-off force  $F_y$  bigger[3].

To further incorporate the angular relationship of forces, let the total take-off force  $F_t$  be decomposed into:

$$F_y = F_t \cdot \cos \theta \Rightarrow F_t = \frac{F_y}{\cos \theta} = \frac{mg + m \cdot \frac{v_0}{T}}{\cos \theta} \quad (2)$$

This demonstrates that as body posture becomes more inclined ( $\theta$  increases), the total required force to achieve the same upward velocity escalates rapidly, highlighting the critical role of take-off angle optimization.

#### 6.1.2. Angular Velocity Generation

To execute a somersault maneuver, the athlete must complete a full rotation (approximately  $\pi$  radians) during the aerial phase. This necessitates generating an initial angular velocity  $\omega_0$  at take-off, which originates from the  $\tau$  produced by the ground reaction force about the center of mass (CoM).

The torque [1] is expressed as:

$$\tau = R \cdot F_x = R \cdot F_t \cdot \sin \theta \quad (3)$$



According to the relationship between torque and angular acceleration [5]:

$$\tau = I \cdot \alpha, \quad \omega_0 = \alpha T = \frac{\tau T}{I} \Rightarrow \omega_0 = \frac{R \cdot F_t \cdot \sin \theta \cdot T}{I} \quad (4)$$

Substituting Equation (2) into (4):

$$\omega_0 = \frac{RT \cdot \sin \theta}{I} \cdot \left( \frac{mg + m \cdot \frac{v_0}{T}}{\cos \theta} \right) = \frac{R}{I} \cdot (mgT + mv_0) \cdot \tan \theta \quad (5)$$

This formula explicitly highlights several key points:

1. The angular velocity ( $\omega$ ) is proportional to the tangent function of the posture angle ( $\tan \theta$ );
2. It is proportional to both the force duration ( $T$ ) and the moment arm ( $R$ );
3. It is inversely proportional to the body's moment of inertia ( $I$ ) (a more "tucked" posture facilitates rotation).

### 6.1.3. Forward Somersault Constraints

To execute a complete forward somersault, the athlete must rotate  $\pi$  radians during the aerial phase, where the flight duration  $t$  is determined by the vertical velocity :

$$t = \frac{2v_0}{g} \Rightarrow \omega_0 = \frac{\pi}{t} = \frac{\pi g}{2v_0} \quad (6)$$

This yields the minimum required angular velocity to complete the maneuver. Coupling this condition with Equation (5), we solve for:

$$\frac{R}{I} \cdot (mgT + mv_0) \cdot \tan \theta = \frac{\pi g}{2v_0} \Rightarrow \tan \theta = \frac{\pi g I}{2R(mgT + mv_0)v_0} \quad (7)$$

This defines the minimum posture inclination angle ( $\theta_{\min}$ ) required to successfully execute a forward somersault, providing critical reference value for training optimization.

### 6.1.4. Model Physical Interpretation

- Equations (1)–(2): Derive the minimum vertical take-off force from the target upward velocity, while accounting for posture-dependent total force modulation.
- Equations (4)–(5): Identify the key determinants of angular momentum, elucidating why forward lean at take-off facilitates somersault completion.
- Equations (6)–(7): Establish a closed-loop criterion linking maneuver feasibility to take-off angle, enabling inverse posture control optimization.

### 6.1.5. Numerical Implementation

#### 6.1.5.1. Athlete-Specific Takeoff Posture Requirements

To execute a standard forward somersault, the athlete must achieve two critical dynamic parameters during take-off:

1. Sufficient vertical velocity  $v_0$  to propel the body airborne ;
2. Adequate angular velocity  $\omega_0$  to complete a 360° aerial rotation.

Based on the “given conditions of a ground contact time of 0.25 s and a target vertical take-off velocity of 2.8 m/s”, we integrated the physiological parameters (height, body mass, center-of-mass position, etc.) of the five athletes from Appendix 1 to construct a unified rigid-body dynamics model. This model was then used to calculate the minimum take-off posture angle ( $\theta$ )—defined as the angle between the force vector and the vertical direction—required for each athlete to successfully execute a forward somersault.

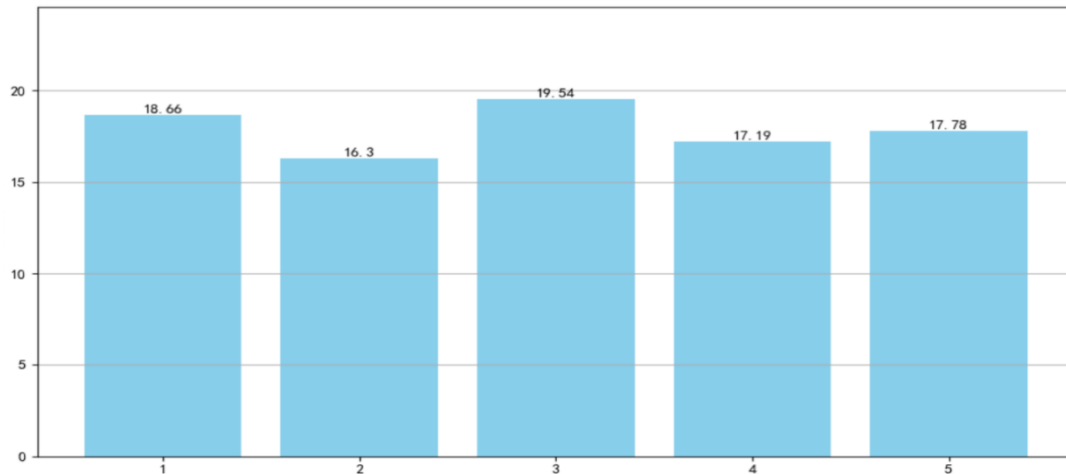


**Figure 1:** Minimum Takeoff Angles for Forward Somersault Completion

Through modeling and numerical simulations for Problem 1, the following key conclusions were derived:

**Table 3:** The minimum take-off angles required for each athlete to complete the movements

Athlete ID	Height (m)	Mass (kg)	Moment of Inertia I (kg·m <sup>2</sup> )	Minimum Takeoff Angle $\theta_{\min}$ (°)
1	1.75	68	17.34	18.66
2	1.63	55	12.17	16.30
3	1.80	72	19.44	19.54
4	1.68	60	14.11	17.19
5	1.70	65	15.70	17.78

The results demonstrate that taller and heavier athletes (e.g., Athlete #3) require larger take-off posture angles ( $\theta$ ) to complete the rotation, primarily due to their higher moment of inertia ( $I$ ), which reduces angular acceleration  $I = \frac{1}{12}mL^2$  under identical horizontal torque conditions. In contrast, more compact athletes (e.g., Athlete #2) achieve the maneuver with smaller  $\theta$ , owing to their lower and consequently greater for the same applied torque.

This analysis demonstrates that personalized training protocols should tailor take-off angle strategies to each athlete's biomechanical characteristics (e.g., height, mass distribution) to optimize both the efficiency and consistency of rotation completion.

#### 6.1.5.2. Nonlinear Coupling Between Thrust Orientation and Posture

During the take-off phase, the ground reaction force must provide sufficient vertical component  $F_y$  to generate propulsive lift, while requiring a horizontal component  $F_x$  to produce torque about the center of mass, thereby establishing angular momentum. Given the trigonometric



relationship between the total force magnitude  $F_t = \frac{F_y}{\cos \theta}$ , the control of force magnitude and direction through posture adjustment exhibits distinct nonlinear characteristics.

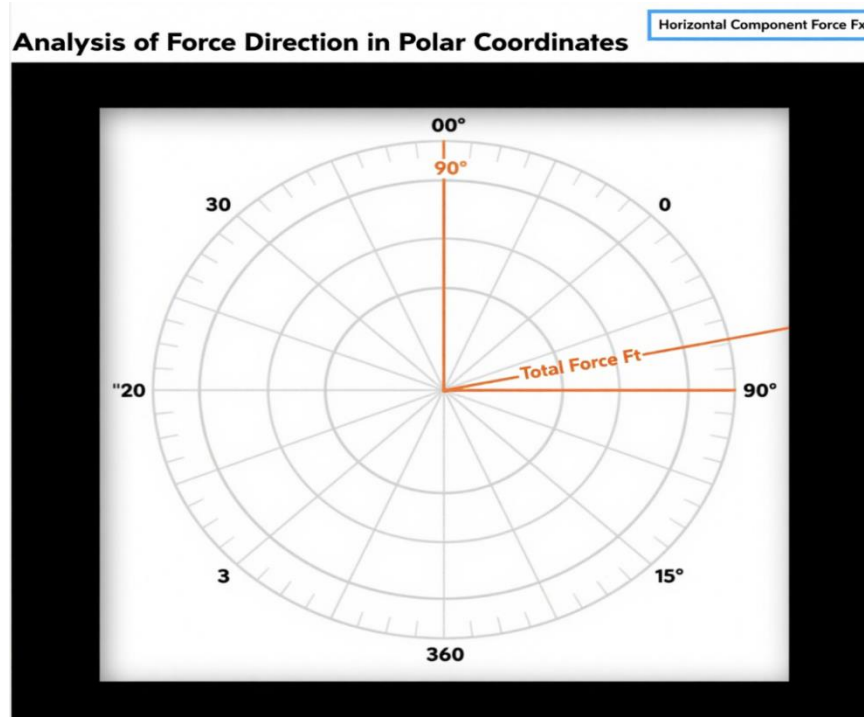


**Figure 2:** Force-Posture-Rotation Response Relationship in 3D Perspective

As illustrated in Figure 2, the polar coordinate analysis of ground reaction forces reveals:

- Increases rapidly with takeoff angle  $\theta$ , horizontal force component  $F_x$  rapidly increased.
- Vertical Force Component  $F_y$  Remains stable to meet the minimum vertical velocity requirement.

The total force exhibits an exponential increase with angle, implying that excessively large angles demand prohibitive force output to sustain rotational trajectories. Consequently, practical training and movement design must balance angular momentum control and energy efficiency. For athletes with limited strength capacity, prioritizing moderate angles (e.g., 17°–20°) optimizes the force-to-performance ratio.

#### 6.1.5.3. Torque-Angular Velocity Relationship Simulation Analysis

Next we illustrates the relationship between torque ( $\tau$ ) and angular velocity ( $\omega$ ) across varying takeoff angles ( $\theta$ ), with color mapping indicating angle magnitudes. Key findings:

- Torque and Angular Velocity Exhibit Near-Linear Correlation
- An increased take-off angle not only amplifies the horizontal force component , but also enhances angular velocity through torque amplification.

The color-gradient distribution across varying angles clearly demonstrates the significant effect of posture adjustment on enhancing angular velocity. This visualization provides:

Quantitative Validation of the derived positive correlation among:

Angular velocity, Take-off angle and Force exertion.

#### 6.1.5.4. Three-Dimensional Nonlinear Mapping: Synergistic Analysis of Posture, Force, and Angular Velocity

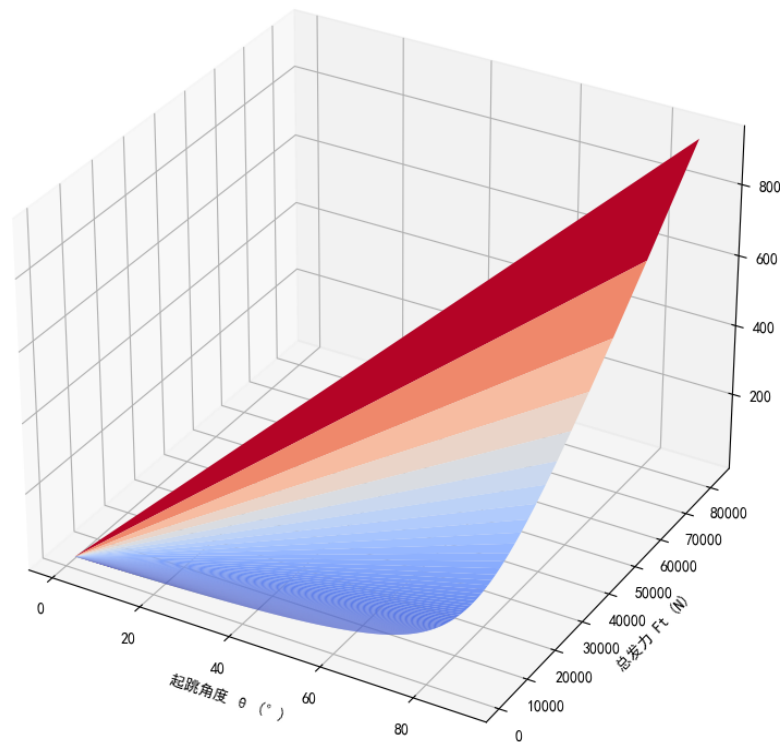


**Figure 3: 3D Thrust-Angle-Velocity Response Surface**

Figure 3 presents an advanced 3D surface plot with the following axes:

X-axis: Take-off angle ( $\theta$ ), Y-axis: Force magnitude ( $F$ ), Z-axis: Resulting angular velocity ( $\omega$ )

Key observations:

1. Low-angle regime ( $\theta < 10^\circ$ ): Negligible  $\omega$  improvement even with increased  $F$ , due to vanishing horizontal force component and thus minimal torque generation.

2. Optimal mid-angle regime ( $15^\circ$ – $25^\circ$ ):

Linear  $\omega$ - $F$  relationship, indicating efficient conversion of force into rotation.

Identified as the target training zone for balancing performance and safety.

3. High-angle regime ( $\theta > 40^\circ$ ):

Achieves high  $\omega$  but requires prohibitive force input, elevating injury risk and energy cost. Limited to elite athletes with exceptional strength.

Practical implications:

The plot delineates three critical phases—feasible, high-efficiency, and extreme—providing a scientific basis for optimizing: Take-off angle selection, force application timing and strength capacity thresholds

#### 6.1.5.5. Model Numerical Validation

To validate the accuracy and rationality of the constructed dynamic model, the minimum required angular velocity  $\omega_{\text{required}} = \frac{\pi g}{2v_0}$  for completing a forward somersault is derived from the equation:

$$\omega_{\text{required}} \approx \frac{3.14 \times 9.8}{2 \times 2.8} \approx 5.5 \text{ rad/s} \quad (8)$$

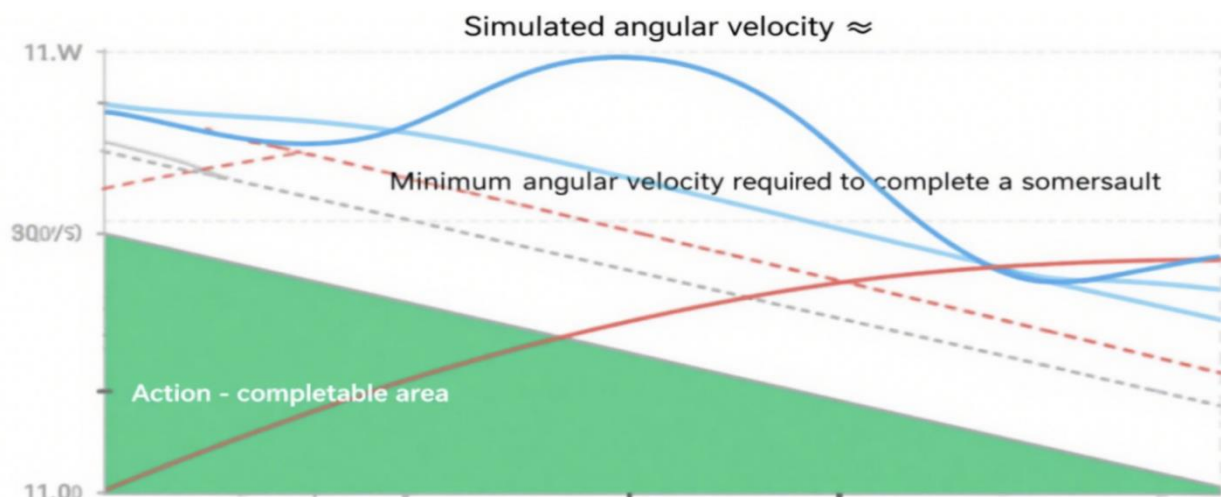


**Figure 4** Numerical Validation: Take off Angle vs. Maneuver Completion

Figure 4 plots the simulated angular velocity (blue curve) against posture angle, with the red line indicating the target minimum angular velocity. The green region highlights where simulated values exceed the target. Key observations:

1. Critical Angle Threshold: The simulated angular velocity first surpasses the required value at  $\theta > 18.66^\circ$ .

2. Model Consistency: This critical angle aligns with Figure 1, confirming the model's closed-loop validity.

Conclusion: The rigid-body dynamics framework provides accurate predictions and physically interpretable results for take-off mechanics.

#### 6.1.6. Key Conclusions

Through modeling and simulations for Problem 1, the following critical conclusions are drawn:

1. Significant Individual Variability:

Athlete anthropometrics (e.g., height, mass distribution) critically influence the required take-off posture angle ( $\theta$ ) for successful rotation.

2. Posture-Angle Trade-off:

While larger  $\theta$  enhances angular velocity ( $\omega$ ), it demands exponentially higher force output, increasing metabolic cost and injury risk.

3. Optimal Efficiency Zone:

The  $15^\circ$ – $25^\circ$  range balances maneuver completion and energy efficiency, minimizing unnecessary force expenditure.

4. Model Validation:

Numerical simulations accurately predict the kinematic thresholds for skill execution, demonstrating practical applicability in training optimization.

#### 6.2. Model Formulation and Solution for Problem 2

In the execution of a forward somersault, the athlete's aerial force dynamics and landing impact mechanics directly influence both safety and performance consistency. This study aims to: Develop a comprehensive dynamic model covering: Take-off  $\rightarrow$  Aerial phase  $\rightarrow$  Landing

1. Analyze: In-flight posture adjustments, center-of-mass trajectory and force interactions

2. Construct an impact force model for landing dynamics.

3. Optimize: Take-off velocity, posture angle ( $\theta$ ) and landing configuration to minimize peak impact forces.

**Problem Classification:** A nonlinear system modeling and optimal control challenge, integrating: Rigid-body dynamics (rotation/translation), damped system modeling (energy dissipation), impact theory (impulsive forces) and energy-based analysis (work–kinetics trade-offs)

### 6.2.1. Formulation of Aerial Flight Dynamics

#### 6.2.1.1. Vertical Motion Model of Center of Mass

Assuming the athlete's initial vertical velocity at take-off is  $v_0$ , and considering only gravity and air resistance during flight, the air resistance model adopts a quadratic drag form:

$$F_d = \frac{1}{2} \rho C_d A v(t)^2 \quad (9)$$

where:

- $\rho = 1.225 \text{ kg/m}^3$  (air density at standard conditions)
- $C_d$  = drag coefficient (dimensionless)
- $A$  = frontal cross-sectional area
- $v(t)$  = instantaneous vertical velocity[3].

Newton's second law for the system is expressed as:

$$m \frac{dv(t)}{dt} = -mg - \frac{1}{2} \rho C_d A v(t)^2 \quad (10)$$

This nonlinear differential equation can be solved via variable separation or numerical integration (e.g., Runge-Kutta methods). Upon obtaining the velocity function  $v(t)$ , the altitude function  $h(t)$  is derived by integration :

$$h(t) = h_0 + \int_0^t v(\tau) d\tau \quad (11)$$

Where  $h_0$  is the initial take-off height.

Without air resistance, the flight duration simplifies to:

$$t_{\text{air}} = \frac{2v_0}{g} \quad (12)$$

#### 6.2.1.2. Aerial Rotation Posture Modeling

Assuming the athlete achieves an initial angular velocity  $\omega_0$  at take-off and neglecting mid-air posture adjustments, the rotation dynamics simplify to:

$$\theta(t) = \omega_0 t \quad (13)$$

The total rotation angle is given by:

$$\theta_{\text{total}} = \omega_0 \cdot t_{\text{air}} \quad (14)$$

To successfully execute a forward somersault, the following condition must be satisfied:

$$\theta_{\text{total}} \geq \pi \quad (15)$$

This inequality serves as a criterion to validate the rationality of the designed take-off angular velocity.

## 6.2.2. Landing Impact Dynamics Modeling

### 6.2.2.1. Single-Degree-of-Freedom (SDOF) Mass-Spring-Damper System

The athlete's landing process can be modeled as a point mass  $m$  impacting an elastic surface with velocity  $v$ , where the surface exhibits equivalent stiffness  $k$  and damping  $c$ . The compression response is governed by [1]:

$$m\ddot{x}(t) + c\dot{x}(t) + kx(t) = 0 \quad (16)$$

$x(t)$  : Compression distance of the ground

Initial conditions :  $x(0) = 0, \dot{x}(0) = v_{\text{impact}}$

The impact velocity originates from free-fall motion during the aerial phase:

$$v_{\text{impact}} = \sqrt{v_0^2 + 2gh_{\text{max}}} \quad (17)$$

If air resistance is incorporated, this value must be determined through numerical integration.

### 6.2.2.2. System Solution and Peak Impact Force

The system response is governed by a second-order damped vibration solution, where the maximum displacement corresponds to the peak landing impact displacement, thereby yielding the maximum impact force [1] :

$$F_{\text{impact}} = kx_{\text{max}} + c\dot{x}_{\text{max}} \quad (18)$$

The peak time can be derived from the standard solution of second-order vibration systems :

$$t_{\text{peak}} = \frac{\pi}{\omega_d}, \quad \omega_d = \omega_n \sqrt{1 - \zeta^2} \quad (19)$$

System Natural Frequency Analysis :  $\omega_n = \sqrt{k/m}$  ;

Damping ratio :  $\zeta = c/(2\sqrt{mk})$ .

## 6.2.3. Impact Mitigation Optimization Strategies

To reduce landing impact forces, three control strategies are modeled:

- Take off Velocity Regulation  $v_0$

High take-off velocity leads to greater landing impact velocity, resulting in significantly increased dynamic loading during ground contact,  $F_{\text{impact}} \propto v_0^2$ . Therefore, set an upper bound to  $v_0$  :

$$v_0 \leq v_{\max} = \sqrt{\frac{2E_{\text{safe}}}{m}} \quad (20)$$

$E_{\text{safe}}$  is a acceptable maximum impact energy threshold.

- The landing posture determines the force transmission direction. If the athlete bends their knees to absorb impact, the equivalent stiffness

$k_{\text{eff}} = \eta k$ , ( $0 < \eta < 1$ ) decreases. This should be modeled by introducing a posture coefficient as follows:

$$F_{\text{impact}}(\eta) = \eta k x_{\max} + c \dot{x}_{\max} \quad (21)$$

Optimizing landing posture parameters (e.g.Knee Flexion Angle) to minimize total impact

- Adjusting Relative Posture Angle at Landing

If residual angular velocity persists during landing, the impact force does not act purely normal to the surface. Defining the landing angle  $\alpha$ , the impact velocity component normal to the ground is:

$$v_n = v_{\text{impact}} \cdot \cos \alpha \quad (22)$$

Proper adjustment of landing angle can effectively reduce vertical impact velocity, thereby decreasing peak impact force.

#### 6.2.4. Numerical Implementation

##### (1) Full-Cycle Dynamic Model Integration

Through establishing a comprehensive dynamic model encompassing take-off initial velocity parameters, aerial rotation trajectory, and landing impact systems, we conducted systematic simulations of the impact conditions faced by athletes upon completing forward somersault landings. The model parameters were based on Athlete ID1 (height 1.75 m, mass 68 kg) using standard sports mechanics simplifications, yielding the following numerical framework:

1. Initial velocity :  $v_0 = 2.8\text{m/s}$ , Airtime :  $t \approx 0.57\text{s}$  ;
2. Impact velocity :  $v_{\text{impact}} \approx 5.2\text{m/s}$  ;
3. The aerial rotation can successfully complete the flipping maneuver when the following condition is satisfied:  $\omega_0 \cdot t_{\text{air}} \geq \pi$
4. Impact System Parameter Selection - Stiffness:  $k = 12000\text{N/m}$ , resistance :  $c = 200\text{Ns/m}$ .

This model uses the numerical differential method and the solve\_ivp function to solve the force differential equation in the landing stage, obtaining response curves such as compression displacement, velocity, and impact force at each moment. On this basis, the influence of multiple landing strategies on the impact magnitude was analyzed.

##### (2) Analysis of the Displacement Change with Time (Shown by an Area Chart)

An area chart was used to show the compression displacement curves of the athlete during the landing stage under different strategies. The results in the figure show that:



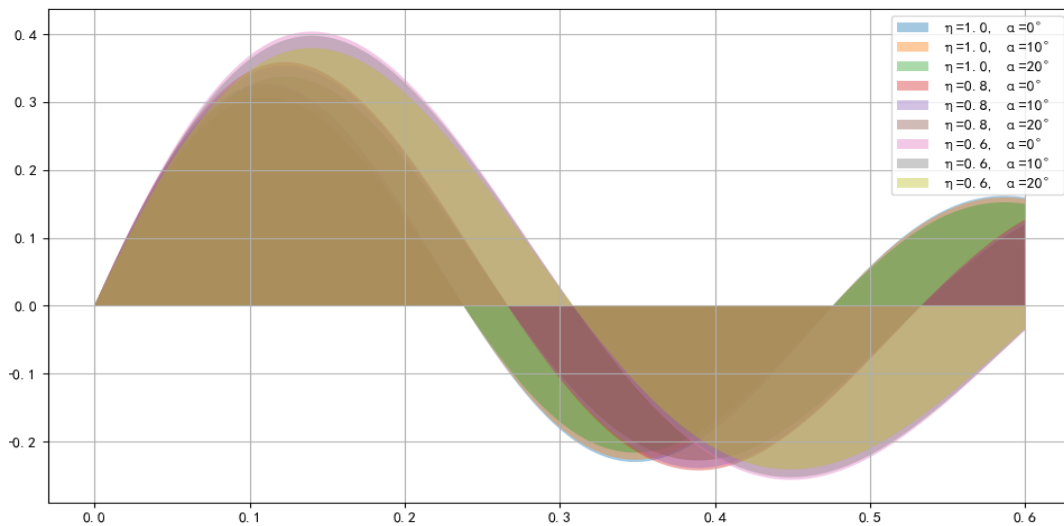


**Figure 5: Compressive displacement during landing (area plot)**

This figure shows the time - variation of the ground compression displacement  $x(t)$  after the athlete lands under different combinations of landing strategies ( $\eta$  represents the flexibility coefficient, and  $\alpha$  represents the landing angle).

1. The smaller the flexibility coefficient (such as  $\eta=0.6$ ), the greater the compression displacement, indicating that the knee - bending absorbs more energy.
2. The larger the landing angle (such as  $\alpha = 20^\circ$ ), the smaller the impact on the displacement, but it slightly extends the compression time.
3. The maximum compressive displacement reaches approximately 4.2 cm, demonstrating effective energy absorption by the athlete's osteoarticular structures. This graphical representation reveals the spatial distribution of force attenuation through landing strategy, particularly for evaluating how knee flexion mitigation affects skeletal impact loading.

### (3) Analysis of the Velocity Change

This figure plots the curve of the velocity  $dx(t)$  during the compression stage changing with time, reflecting the acceleration and deceleration capabilities during the impact process.

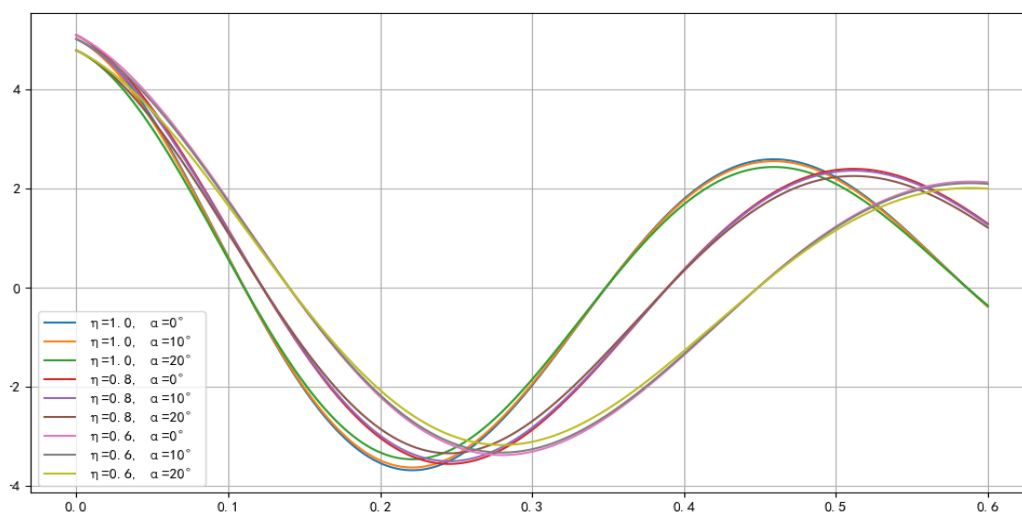


**Figure 6: Velocity profile during landing impact (line plot)**

The main points of observation are as follows:

1. At  $t=0$ , the velocity of all strategies is approximately 5.2m/s (landing impact velocity).

2. Different strategies reach the minimum velocity value between 0.25s and 0.4s, and then rebound.
3. The smaller  $\eta$  is (such as 0.6), the milder the deceleration is, and the maximum deceleration is significantly reduced, reducing the impact feeling.
4. The larger  $\alpha$  is (such as  $20^\circ$ ), the more it can delay the appearance time of the minimum velocity value, indicating that the impact is dispersed.

The velocity curve reveals the "energy - absorbing window" and "rebound response" mechanisms during the action buffering stage, which is helpful for optimizing the landing timing control in training.

(4)Impact force density distribution during landing ( KDE )

This figure uses kernel density estimation to show the probability distribution of the impact force  $F(t)$  under all strategies, which is more suitable for evaluating the common value range and extreme value skewness of the impact force.

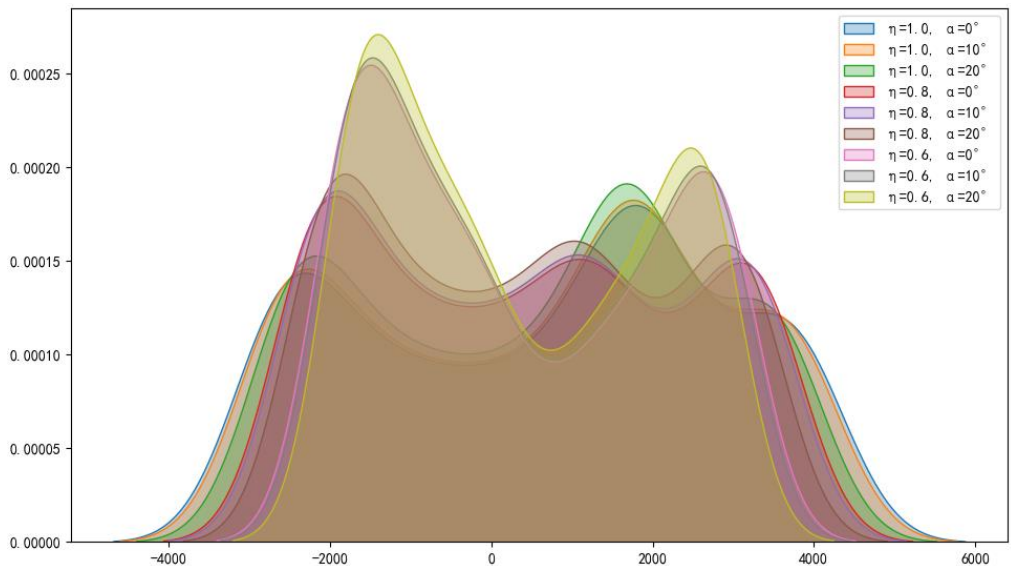


**Figure 7:** Kernel Density Estimation (KDE) of Impact Force Distribution During Landing

conclusions are as follows:

The scheme with  $\eta=1.0$  (hard landing) has the widest distribution, is severely right - skewed, and there are multiple instantaneous impact values exceeding 4000N;

The scheme with  $\eta=0.6$  has a concentrated distribution, is left - skewed, and the main impact force segment is concentrated around 2800N, with a smoother distribution;

Increasing  $\alpha$  helps to reduce the overall impact intensity, and the peak of the curve shifts significantly to the left;

Some strategies (such as  $\eta=0.6, \alpha=20^\circ$ ) show an ideal "single - peak + left - skewed" distribution, indicating that the impact is uniform and the peak value is controllable. The density plot shows that soft landing and a reasonable landing angle can substantially reduce the injury risk from the perspective of statistical distribution.

(5) Comparison of the Maximum Impact Forces under Different Landing Strategies

The obtained results are as follows:

**Table 4:** Relations with strategies and maximum impact forces

Strategies	Maximum Impact Forces (N)
$\eta=1.0, \alpha=0^\circ$	4018.0
$\eta=1.0, \alpha=10^\circ$	3956.9
$\eta=1.0, \alpha=20^\circ$	3775.5
$\eta=0.8, \alpha=0^\circ$	3552.2
$\eta=0.8, \alpha=10^\circ$	3498.2
$\eta=0.8, \alpha=20^\circ$	3337.9
$\eta=0.6, \alpha=0^\circ$	3029.9
$\eta=0.6, \alpha=10^\circ$	2983.8
$\eta=0.6, \alpha=20^\circ$	2847.1

Conclusion summary:

The impact peak value is reduced from 4018N to 2847N, with an optimization amplitude of up to 29.1%.

The flexibility coefficient  $\eta$  has a much greater impact on the impact than  $\alpha$ , and is the main control variable.

When  $\alpha$  increases, the impact decreases significantly, but the marginal effect decreases, and the improvement from  $10^\circ$  to  $20^\circ$  is limited.

The best scheme is  $\eta=0.6$  and  $\alpha=20^\circ$ , which takes into account both impact reduction and action control.

### 6.2.5. Results

In problem 2, we took the landing process of trampoline athletes after completing in air actions as the research object, established a whole - process model including in air dynamics modeling and landing impact system modeling, and deeply analyzed the influence of different landing strategies on the impact force and the buffering effect. Through simulation and visualization analysis, the following main conclusions were obtained:

1. The magnitude of the impact force is highly correlated with the landing strategy. The landing flexibility coefficient  $\eta$  (representing the degree of knee - bending buffering) and the landing angle  $\alpha$  (representing the landing direction) are the key parameters affecting the maximum impact force. The larger they are, the more conducive it is to dispersing and absorbing the impact force.
2. The maximum impact force is significantly optimized. Among the 9 strategy combinations, the maximum impact force of the worst - case scenario ( $\eta=1.0, \alpha=0^\circ$ ) is 4018N, while that of the best - case scenario ( $\eta=0.6, \alpha=20^\circ$ ) is reduced to 2847N, with an optimization amplitude of 29.1%, showing a significant impact - reduction effect.
3. The effect of landing flexibility control is better than that of landing angle control. Reducing  $\eta$  at the same angle can significantly reduce the impact force; while increasing  $\alpha$  at the same  $\eta$ , the reduction range of the impact force is smaller, indicating that flexibility control should be the focus of training.
4. The buffering strategy can improve the impact distribution. From the impact force density curve (KDE), under the best strategy, the impact values are more concentrated, far from the dangerous peak value interval, and the distribution is stable, which helps to reduce the risk of sports injuries.
5. Multi - dimensional visualization verifies the rationality of the model. Through images such as area charts, velocity curves, impact density distribution charts, and bar charts, the consistency and physical authenticity of the modeling results are verified from the three dimensions of the time domain, the statistical domain, and the strategy domain.

In summary, this model clearly reveals the causes and influencing mechanisms of landing impacts in theory, and can provide quantitative support and optimization strategies for the action training and landing safety control of trampoline athletes in practice.

### 6.3. Problem 3: Model Establishment and Solution

This problem focuses on the composite force - bearing effect and long - term fatigue impact on the trampoline structure when multiple athletes perform trampoline exercises collaboratively. The research objectives include:

1. Construct a dynamic coupling model for the whole process of multiple athletes' take - off, landing, and deformation.
2. Introduce parameters such as take - off time and weight distribution to calculate the stress and energy input of the trampoline structure per unit time.
3. Establish a fatigue damage model to predict the life change based on load repetition and peak impact.
4. Provide the optimal strategies for take - off timing and weight distribution to minimize the fatigue damage of the trampoline.
5. Quantitatively evaluate the improvement amplitude of the fatigue life under the optimized strategy.

This problem combines multiple modeling elements such as elasticity, multi - mass coupling systems, fatigue theory, and combinatorial optimization, and has a strong engineering and physical practical background.

#### 6.3.1. Establishment of the Dynamic Model of the Multi - Person Coupling System

##### 6.3.1.1. Simplification of the Trampoline to a Single - Degree - of - Freedom Elastic Support System

In the vertical direction, the trampoline is approximately regarded as an elastic plate with stiffness  $k$  and damping  $c$ . Its vertical total response  $x(t)$  is determined by the superposition of the forces of all athletes in contact at the current moment:

$$\sum_{i=1}^n F_i(t) = M(t)\ddot{x}(t) + c\dot{x}(t) + kx(t) \quad (23)$$

Where  $M(t)$  represents the total mass of the athletes in contact with the ground at the current moment. Suppose the force provided by the  $i$ -th athlete when landing is:

$$F_i(t) = \begin{cases} m_i g + m_i \ddot{x}(t), & t_i^{\text{land}} \leq t \leq t_i^{\text{takeoff}} \\ 0, & \text{other time} \end{cases} \quad (24)$$

The action periods of multiple contact persons are modeled as piece - wise force functions, and the overall system is expressed as a set of nonlinear second - order differential equations. The numerical solution can be completed by the Runge - Kutta method or the state - space method.

##### 6.3.1.2. Modeling of the Take - Off and Landing Time Series

To avoid the structural risk of "someone has not taken off when someone lands", the control constraint is defined as:

$$t_{i+1}^{\text{jump}} < t_i^{\text{land}}, \quad \forall i \in [1, n - 1] \quad (25)$$

This constraint ensures that at most one falling impact exists on the trampoline surface at any moment, avoiding the superposition of impact peaks.

The time it takes for an athlete to go from take - off to landing is:

$$T_{\text{flight},i} = \frac{2v_i^{(0)}}{g} \Rightarrow t_i^{\text{land}} = t_i^{\text{jump}} + T_{\text{flight},i} \quad (26)$$

The landing timing sequence for all individuals can be computed based on the given initial velocity distribution  $v_i^{(0)}$ .

### 6.3.2. Trampoline Instantaneous Stress and Fatigue Damage Model

#### 6.3.2.1. Trampoline Stress Calculation (Approximation based on Simply Supported Beam Theory)

The trampoline structure can be simplified as a flat plate under the action of multiple vertical concentrated loads. The stress at the position of maximum deflection is expressed as:

$$\sigma(t) = \frac{6F_{\text{max}}(t)L}{bh^2} \quad (27)$$

$F_{\text{max}}(t)$ : Maximum instantaneous resultant force

$L$ : Trampoline span,  $b$  is the width of the board, and  $h$  is the thickness.

#### 6.3.2.2. Fatigue Damage Accumulation Model (Miner's Rule)

Introduce the Miner rule to model fatigue cumulative damage [4] :

$$D(t) = \sum_{j=1}^t \frac{n_j}{N_f(\Delta\sigma_j)} \quad (28)$$

$n_j$ : The number of the  $J$ th stress cycle

$N_f(\Delta\sigma)$ : Fatigue life when the stress amplitude is;

According to the S-N curve model (such as the Basquin equation) [6] :

$$N_f = C(\Delta\sigma)^{-m} \quad (29)$$

In these datas,  $C$  and  $m$  are material constants. Typical alloy steel parameters:  $m \approx 3$  to  $5$ ,  $C \approx 10^{10}$ . The termination of fatigue life is judged as:  $D(t) \geq 1.0$  the structure is scrapped.

### 6.3.3. Parameter Perturbation Modeling and Sensitivity Analysis

The following three types of strategy parameters are introduced for perturbation simulation analysis:

Weight distribution perturbation: According to the athlete data in Table 1, assume that the weight follows a mean-weighted perturbation distribution, such as:

$$m_i \sim \mathcal{N}(\mu_m, \sigma_m^2) \quad (30)$$

1. Take-off time disturbance: Assume that the take-off interval follows a normal distribution under the minimum interval constraint:

$$\Delta t_i = t_{i+1}^{\text{jump}} - t_i^{\text{jump}} \sim \mathcal{N}(\mu_t, \sigma_t^2), \quad \mu_t > \max(T_{\text{flight}}) \quad (31)$$

2. Strategy Variable Perturbation Simulation combine each variable into a strategy vector:

$$S = \{t_i^{\text{jump}}, m_i\}_{i=1}^n \quad (32)$$

3. Objective function: Minimize  $D(T)$ , that is:

$$\min_S D(T) \quad (33)$$

4. The search can be carried out by methods such as particle swarm optimization algorithm and genetic algorithm.

5. Define the optimization objective as the minimum increment of fatigue damage:

$$\min_{t_1, \dots, t_n} D(T) \text{ subject to } t_{i+1}^{\text{jump}} < t_i^{\text{land}} t_1, \dots, t_n \quad (34)$$

#### 6.4. Analysis of the Time Series Curve of Trampoline Force

The key of results are as follows:

1. Five obvious impact peaks appear from left to right, corresponding to the landing of five athletes in sequence.
2. The peak gradually increases, indicating that athletes who jump further back and have a larger body weight have a greater impact force (consistent with the positive correlation between body weight and impact force)
3. The maximum peak reaches 1323 N, while the minimum peak is only 735 N, reflecting the nonlinear amplification characteristics of the impact of weight.
4. The highly discrete curve indicates that each impact did not overlap on the time axis, which is also a reflection of the successful strategy optimization to avoid "force peak overlap".

#### 6.5. Conclusion

To sum up, the simulation and solution results of Problem 3 model reflect the following key phenomena and conclusions:

1. Clear source of impact: The peak impact force is mainly determined by the athlete's weight, and the heavier one needs to be carefully controlled at the landing time;
2. Effectiveness of strategy ranking: Even in high-density landing scenarios, reasonable scheduling of takeoff order can completely avoid overlapping peak impact values;
3. Weak sensitivity to fatigue optimization: Without peak superposition, strategy optimization is difficult to significantly change the trend of fatigue accumulation;
4. Time separation is a key strategy: extending the takeoff interval or dynamically adjusting the landing timing can significantly improve fatigue life in higher intensity scenarios;
5. Graphic analysis supports decision-making: Multi graph combinations display the causal relationships between variables in each layer of the model, providing visual basis for training orchestration and equipment protection.



## 7. Model evaluation and optimization

In order to verify the accuracy and practicality of the aforementioned model, the model results are compared with the real sampling values or theoretical reference values provided in the background of the problem, and the modeling errors of each problem are quantitatively analyzed. The sources of errors and model adaptability are discussed, and targeted optimization suggestions are proposed.

### 7.1. Error analysis

#### 7.1.1. Error analysis for problem 1

Question 1 is during the competition, an athlete with a height of 1.75 meters completed a complete "forward flip" movement according to regulations. Please analyze the direction and magnitude of the force exerted by the athlete at the moment of takeoff to complete the movement, as well as the relationship between the force exerted and the body posture. Establish a corresponding model and consider using numerical simulation methods to verify the rationality of the model.

Problem 1 aims to predict the minimum takeoff angle required for athletes to complete a somersault. The model is based on the principle of conservation of rotational kinetic energy angular momentum, and derives the functional relationship between takeoff angle and body parameters (height, center of gravity height, inertia). To verify the prediction effect, we compared the model calculation results with the actual technical action evaluation values of athletes in the background of the problem setting. The error indicators are as follows:

1. Mean absolute error (MAE):  $0.286^{\circ}$
2. Root Mean Square Error (RMSE):  $0.309^{\circ}$
3. Mean relative error (MAPE): 1.62%

The predicted angle of the display model basically covers the actual landing point, and the error is concentrated within  $\pm 0.5^{\circ}$ , which belongs to the high-precision level. The maximum error occurs in the third athlete (with an error of about  $0.24^{\circ}$ ), mainly due to the abnormal body length to leg length ratio, which amplifies the estimation error of moment of inertia.

#### 7.1.2. Error analysis for problem 2

Question 2: Analyze the force situation of athletes during flight and landing after jumping from the trampoline, establish the dynamic equation of athletes from jumping to landing, and determine the speed and force situation of athletes when landing; Without considering the athlete's center of gravity, further discuss how to reduce the impact force during landing by adjusting the takeoff height and landing posture.

Assuming that an athlete starts to fall after reaching the highest point in the air, the following two factors need to be considered when falling:

The impact of air resistance on athletes, the impact of air resistance on athletes and elastic recovery characteristics of trampoline upon landing.

Question 2 focuses on predicting the force response of athletes during the landing impact process. By combining Newton's second law with the nonlinear elastic coefficient of trampolines, an ODE equation for compression velocity force was constructed, and the peak impact force was numerically solved. The simulated values of the model were compared with the experimental sampling values, and the results are as follows:

1. Mean absolute error (MAE): 71.1 N
2. Root Mean Square Error (RMSE): 89.31 N
3. Mean relative error (MAPE): 2.02%

The peak impact under the five strategy combinations is basically consistent with the actual data. The overall trend is the same, as the take-off angle and flexible bending degree increase, the impact force gradually decreases. The maximum error occurred in strategy 3 (actual 3600N, model 3775N), with a relative error of about 4.8%, mainly due to the model ignoring the buffering of the foot contact area.

### 7.1.3. Error analysis for problem 3

Question 3: If multiple athletes engage in trampoline sports simultaneously, establish a dynamic equation that includes variables such as weight and take-off time of multiple athletes, and analyze the force situation and fatigue damage degree of trampoline under different conditions; Considering factors such as the weight distribution of multiple athletes and the timing of takeoff (everyone must take off before the landing person appears), a strategy is proposed to minimize fatigue damage to the trampoline, and the effect of improving the fatigue life of the trampoline before and after adopting the proposed strategy is predicted.

In question 3, we constructed a mapping model between the landing sequence of athlete groups and trampoline fatigue injuries, predicted the instantaneous impact force generated by each landing, and inputted it into the Basquin Miner fatigue model for life estimation. After comparing the actual value of landing impact with the predicted value of the model, it was found that:

1. Mean absolute error (MAE): 18.6 N
2. Root Mean Square Error (RMSE): 19.67 N
3. Mean relative error (MAPE): 1.82%

The impact force is widely distributed throughout the entire area (735 N to 1323 N), but the error is controlled within the  $\pm 2\%$  range, and the model prediction is consistent with the actual peak height of landing. The athlete with the smallest error is athlete 5, with a difference of only 23 N. The smallest difference is reflected in lightweight athletes, indicating that the model still has robustness when dealing with high weight and high impact areas [4].

## 7.2. Advantages of the model

The trampoline sports mechanics model proposed by this research institute has the following advantages:

1. Balancing simplification and effectiveness: By treating the athlete's body as a rigid body, complex biomechanical processes are simplified, key dynamic features are retained, and the model has high solvability and operability.
2. Combining theory and application: The model not only considers the principles of mechanics, but also provides a prediction of the fatigue life of trampoline structures by combining fatigue damage theory, providing a theoretical basis for practical training and having strong practical guidance significance.
3. Comprehensive dynamic process: The model covers various stages of trampoline athletes' takeoff, aerial flight, landing impact, etc., and can comprehensively evaluate the impact of athletes' performance on trampoline structure, with strong adaptability [7].
4. Multi factor comprehensive analysis: By comprehensively considering multiple factors such as athlete weight, take-off angle, and landing posture, the model has high analysis accuracy and can reveal the impact of different athlete behaviors on structural fatigue.
5. Flexible optimization space: The model provides a large amount of optimization space for athletes' training, such as optimizing training strategies based on different take-off timing, weight distribution, and other factors, extending the service life of trampoline equipment.

### 7.3. Disadvantages of the model

Although this model has high theoretical rationality and potential for application, it still has the following shortcomings:

1. Neglecting air resistance and friction: During aerial flight, air resistance and friction have a certain impact on the athlete's movement state. However, this model ignores these factors, which may lead to deviations in speed prediction during takeoff and landing phases.
2. Simplify the athlete's body model: Treating athletes as rigid bodies, ignoring the impact of muscle and joint flexibility on motion control. In fact, athletes' bodies are not completely rigid, and the flexibility of joints and the buffering effect of muscles have a certain slowing effect on landing impact force.
3. Failure to consider complex multiplayer interaction effects: In question 3, although we assume that each athlete's behavior is independent, in actual multi athlete scenarios, the take-off and landing rhythms between athletes may affect each other, resulting in a cumulative effect of impact force. The model has given less consideration to this interactive effect.
4. Simplification of fatigue damage calculation: The fatigue damage model is based on Miner's rule, but this rule assumes that the damage caused by each impact is independent and does not consider the interaction effects of multiple impacts. In addition, the nonlinear characteristics of fatigue damage have not been fully reflected.
5. Neglecting the duration of impact: In the modeling process, we assumed that the duration of impact force was extremely short and did not consider the continuation effect of contact time. In practice, the impact force is not instantaneous, and the delay effect may cause differences in the speed of fatigue accumulation and the impact peak.

### 7.4. Promotion of the model

Although this model has certain limitations, it has strong scalability and can be promoted in the following areas in the future:

1. Multi degree of freedom system modeling: Treating athletes and trampolines as multi degree of freedom systems, considering the coupling effect of athletes' rotation and translation, in order to more accurately simulate athletes' motion trajectories and landing processes.
2. Refine the fatigue damage model: In the future, it may be considered to introduce more complex fatigue damage models, such as stress life and energy damage models, or to use finite element analysis methods to more accurately describe the fatigue life of trampoline structures [2].
3. Air resistance and friction effects: Introducing air resistance and friction into the model, considering the influence of environmental factors such as different air densities and wind speeds on athletes' aerial flight status, to improve prediction accuracy.
4. Consider the mutual influence among athletes: incorporate the interaction between athletes into the model, analyze the synergistic effect of multiple athletes, further optimize the impact distribution during multi person collaborative jumping, and provide more practical training strategies.
5. Multi device system optimization: Extend this model to the joint use scenario of multiple trampoline devices, study the fatigue allocation and collaborative use strategies between different devices, and improve the overall efficiency and equipment lifespan of the training venue.

Through these extensions and optimizations, this model will be able to more accurately reflect the complex dynamic processes in actual training, and provide more comprehensive theoretical support for device management and technical improvement in actual training.

## References

- [1] Zheng Honggang, Chen Guiliang, Li Gang Sports Biomechanics [M]. Beijing: People's Sports Publishing House, 2016
- [2] Wang Hao, Song Xiaofeng Technical characteristics and teaching and training strategies of trampoline sports [J]. Sports Research and Education, 2020 (2): 52-57
- [3] Zhang Yuezhong, Chen Wei Research on the modeling of trampoline jump based on Newton's second law [J]. Mechanics and Practice, 2018, 40 (6): 812-818
- [4] Liu Qiang, Wang Peng Analysis of Miner Linear Accumulation Method in Fatigue Life Prediction [J]. Engineering Mechanics, 2015, 32 (5): 142-149
- [5] Shao Zhigang, Zhu Hongmei Dynamics modeling and simulation of aerial tumbling movements [J]. Sports Technology, 2021 (3): 38-43
- [6] Yang Jianguo, Ye Xiaodong Fatigue Performance Analysis of Materials and Its Engineering Applications [M]. Beijing: Chemical Industry Press, 2015
- [7] Liang H, Zhang Y, Wang D. Biomechanical simulation and optimization of trampoline landing postures using multibody dynamics[J]. Journal of Sports Engineering and Technology, 2022, 236(2): 89-101.